Journal of Applied Physics

RESEARCH ARTICLE | MARCH 01 2022

Condensation of 2D exciton-polaritons in an open-access microcavity

Feng Li ; Yiming Li; L. Giriunas; M. Sich ; D. D. Solnyshkov ; G. Malpuech; A. A. P. Trichet; J. M. Smith ; E. Clarke ; M. S. Skolnick; D. N. Krizhanovskii

Journal of Applied Physics 131, 093101 (2022)
https://doi.org/10.1063/5.0076459

AIP Publishing

Journal of Applied Physics ARTICLE scitation.org/journal/jap

Condensation of 2D exciton-polaritons in an open-access microcavity

Cite as: J. Appl. Phys. **131**, 093101 (2022); doi: 10.1063/5.0076459
Submitted: 25 October 2021 · Accepted: 9 February 2022 ·
Published Online: 1 March 2022

View Online Export Citation CrossMark

Feng Li,[1,2,a] Yiming Li,[1] L. Giriunas,[2] M. Sich,[2] D. D. Solnyshkov,[3,4] G. Malpuech,[3] A. A. P. Trichet,[5] J. M. Smith,[5] E. Clarke,[6] M. S. Skolnick,[2] and D. N. Krizhanovskii[2]

AFFILIATIONS

[1]Key Laboratory for Physical Electronics and Devices of the Ministry of Education & Shaanxi Key Lab of Information Photonic Technique, School of Electronic Science and Engineering, Faculty of Electronic and Information Engineering, Xi'an Jiaotong University, Xi'an 710049, China
[2]Department of Physics and Astronomy, The University of Sheffield, Sheffield S3 7RH, United Kingdom
[3]Institut Pascal, PHOTON-N2, Université Clermont Auvergne, CNRS, 4 Avenue Blaise Pascal, 63178 Aubière Cedex, France
[4]Institut Universitaire de France (IUF), 75231 Paris, France
[5]Department of Materials, University of Oxford, Oxford OX1 3PH, United Kingdom
[6]EPSRC National Centre for III-V Technologies, University of Sheffield, Sheffield S1 3JD, United Kingdom

[a]**Author to whom correspondence should be addressed:** felix831204@xjtu.edu.cn

ABSTRACT

We establish a tunable open-access microcavity consisting of two planar distributed Bragg reflectors (DBRs) individually controlled by nanopositioners. By varying the cavity length, such configuration enables variation of the light–matter coupling strength by a factor of 2, while keeping in microresonators the same active region and cavity mirrors. Polariton condensation was demonstrated over a large range of Rabi splittings and the corresponding threshold diagram was derived as a function of cavity-exciton detuning, which fits well with theoretical simulations. The results show that for various light-matter coupling strengths, optimal detunings featured by the lowest condensation threshold always occur at a fixed depth of energy trap between the exciton reservoir and the polariton ground state, which enables the most efficient exciton–exciton scattering into the condensate state in the driven-dissipative polaritonic system.

I. INTRODUCTION

Microcavities, being able to confine light down to the wavelength scale, have been developed as an important tool to enhance the light–matter interaction.[1–3] A microcavity with an embedded optically active region can work either in the strong or in the weak coupling regime depending on a number of factors including light–matter field overlap, emitter oscillator strength, cavity quality factor, etc.[4,5] In the strong light–matter coupling regime, Bose–Einstein condensation (BEC) of cavity polaritons was demonstrated due to their Bosonic nature,[6] forming on-chip quantum fluid of light.[3] In the driven-dissipative system of polaritons, the interplay between kinetics and thermodynamics determines a condensation threshold diagram that displays the condensation threshold power as a function of cavity-exciton detuning, in which an optimal detuning corresponding to the lowest threshold can be identified.[7–10] By far, the way to obtain the condensation phase diagram is varying the cavity-exciton detuning. However, this process changes simultaneously several factors that affect the condensation threshold and thereby makes it difficult to study the role of each factor individually. For example, when the cavity-exciton detuning is changed, the particle properties of polaritons (i.e., polariton mass and lifetime) change together with the depth of the potential trap [i.e., the energy difference between the exciton reservoir and the bottom of the lower polariton branch (LPB)], while both of them affect the condensation mechanism but cannot be analyzed independently.[11] This issue, nevertheless, can be well addressed with a large range of tunability of the light–matter interaction strength, i.e., the vacuum Rabi splitting of the system. For example, by fixing the energy of LPB bottom and varying the value of Rabi, one can change the polariton mass and lifetime while keeping the same depth of potential trap.

The continuous tunability of light–matter coupling strength in a large range can be achieved by varying the cavity length that would cover many optical half wavelengths, which changes the mode volume and thereby alters the optical field overlap with the emitter.[4,12,13] Although such large range of cavity length tunability is difficult for monolithic microcavities, it is fully realizable in the recently developed open-access microcavity, which consists of two distributed Bragg reflectors (DBRs) separated by a micro-sized air-gap and controlled individually by nanopositioners so that the cavity length can be flexibly tuned.[14–17] In the concave-planar cavity structure supporting zero-dimensional (0D) polaritons, the maximum allowed cavity length is determined by the radius of curvature (RoC) of the concave mirror, while a planar–planar cavity structure would, in principle, support two-dimensional (2D) polaritons with a cavity length up to infinity. Such mechanism exhibits the advantage of tuning light–matter coupling while keeping both the physical properties of the emitter and the cavity mirror loss unchanged, providing possible opportunities for an easy control of light confinement and propagation on a micrometer length scale. 2D polaritons in open-access microcavities have been demonstrated with organic and monolayer emitters[18,19]; nevertheless, the momentum space imaging and polariton condensation have not been studied yet in such systems.

In this article, we report on the condensation of 2D exciton–polaritons in a tunable microcavity over a large range of Rabi splittings from ∼7 to ∼13 meV, which was enabled by varying the distance between the two mirrors in open-access microcavities from a few to tens of micrometers. Polariton condensation threshold diagrams were derived at various exciton–photon detunings and Rabi splittings, which showed that, regardless of the polariton mass and lifetimes of the condensed state, optimal detunings always correspond to a fixed depth of potential trap in momentum space. The results highlight the significant role played by the polariton potential trap and exciton-pair scattering in the non-equilibrium condensation process,[11] which agree well with theoretical simulations of kinetics vs thermodynamics.

II. SAMPLE PREPARATION AND EXPERIMENTAL SETUP

The configuration of the open microcavity system is based on the setup already reported in Ref. 16. A semiconductor half-cavity and a dielectric DBR are controlled individually to form the open-access cavity, as illustrated in Fig. 1(a). The semiconductor half-cavity consists of 30 pairs of $Al_{0.2}Ga_{0.8}As/Al_{0.95}Ga_{0.05}As$ DBR and on top a 2λ-cavity region with three sets of four GaAs multiple quantum wells (MQWs) embedded at the expected optical field antinodes. The dielectric DBR is fabricated by depositing 11 pairs of SiO_2/Ta_2O_5 quarter-wavelength bilayers on the surface of a plinth sized $200\,\mu m^3$ fabricated on the silica substrate, as illustrated in Figs. 1(b) and 1(c). Unlike the previously reported open microcavities that have at least one concave mirror,[16,17,20,21] the planar open-access cavity requires perfect angular alignment between the semiconductor and dielectric DBRs to keep them extremely parallel. To achieve this, two high-resolution Attocube goniometers were used to make two-dimensional adjustment of the tilt angle of the semiconductor DBR according to the measured energy–momentum (E–k) images in realtime and essentially have it parallel with

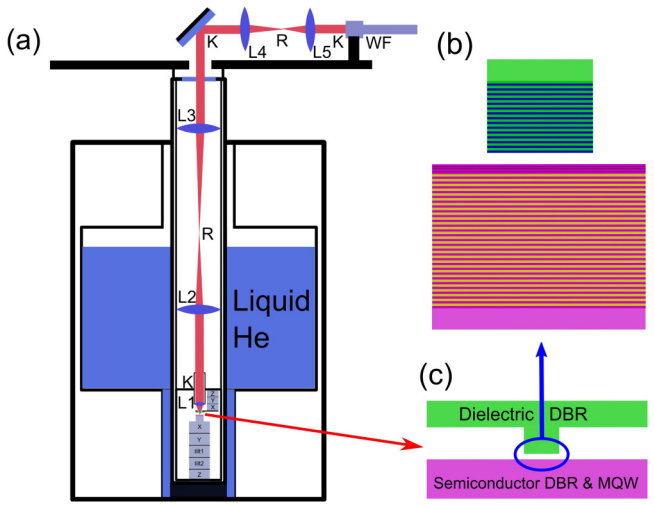

FIG. 1. (a) Illustrative diagram of the angular resolved spectroscopy setup for open microcavities. Focal length for lenses: L1 7.5 mm, L2 300 mm, L3 500 mm, L4 200 mm, and L5 50 mm. WF stands for wound fiber. R and K stand for the positions of real space and k-space images, respectively. (b) and (c) Zoomed-in pictures of the cavity part.

the dielectric DBR. Another requirement for the planar open-access cavity is high mechanical stability. Touching the two DBRs mechanically, which is the commonly used method for stabilizing planar–concave open cavities, cannot be applied to the planar–planar open-access cavity as it destroys the parallelism. To gain better stability, the liquid helium Dewar that hosts the system is placed on a air-inflated floating cradle, and the entire setup, including the Dewar and the optics on it, is enclosed by acoustic foams.

The setup of angular resolved spectroscopy is built with five confocal lenses, two of which are mounted inside the helium Dewar, as shown in Fig. 1(a). The excitation beam travels through L3 and L2 and is focused onto the open-access cavity by L1 (focal length 7.5 mm, numerical aperture 0.32). The emission is collected by L1 and the k-space image is transferred by L2–L5 and projected on a wound fiber (WF) bundle, which sends the image to the spectrometer and CCD.

III. RESULTS AND DISCUSSION

The effective length of the cavity in resonance with the exciton in QW can be written as $L_{\text{eff}} = (l+4)\lambda_X/2 + L_{\text{DBR}}$, where $\lambda_X = 770$ nm is the exciton emission wavelength and L_{DBR} is the penetration length of the optical field into the DBRs. Here, we define the dimensionless integer l as the longitudinal order of the cavity. A continuous Ti:sapphire laser, tuned to the first Bragg mode of the dielectric DBR at the wavelength of 739 nm, is used to excite the free carriers in the quantum wells embedded in the open-access cavity with a spot size of $\sim 50\,\mu m$. It is noted that the center wavelength of the dielectric DBR stopband, which is ∼150 nm wide, is intentionally designed at a larger wavelength of ∼843 nm than λ_X to allow the pump laser to pass at the wavelength of the

Bragg mode. The energy–momentum (E–k) images of 2D polaritons are shown in Fig. 2(a) for $l = 5$, 29, and 51 (herein $l = 0$ corresponds to the situation that the two mirrors touches), in which the lower polariton branch (LPB) and the upper polariton branch (UPB) are seen for each l. The cavity-exciton detunings are all tuned so that the bottoms of the LPB are at the same energy of 1602 mev (774 nm). As the field overlap between the cavity mode and the exciton decreases with l, the Rabi splitting decreases and the LPB becomes more photonic like. The exciton–photon detunings are +1.68, −1.21, and −2.61 meV for ls of 5, 29, and 51, respectively. A second LPB very negatively detuned with respect to the exciton resonance corresponding to a lower longitudinal cavity mode order also appears for $l = 29$ and $l = 51$ due to the reduced free spectral range. Although the Rabi splitting can be roughly derived from the minimum separation between the LPB and the UPB in E–k dispersion [red arrows in Fig. 2(a)], we adopted a more precise method for obtaining the Rabi-splitting. For each l, we take the spectra at $k = 0$ while continuously decreasing the cavity length with the applied voltage on the nanopositioner as reported in Ref. 16 and obtain the minimum separation between the LPB and the UPB. Figure 2(b) shows the measured Rabi splitting as a function l, which can be fitted with $\Omega_{Rabi} \propto 1/\sqrt{L_{\text{eff}}}$ as expected.[16] Polariton condensation was observed for each l by increasing the pump power, featured by the polariton blueshift which, though showing fluctuations vs l, is always much smaller than the energy difference between the bare cavity mode and the LPB bottom $E_{Cav} - E_{LPB}$, as plotted in Fig. 2(c). The blueshift is given purely by interaction with the exciton reservoir,[22,23] and the density of which is given by the value of the pump power absorbed. This provides a way to explore the unique advantages of using long cavities for polariton studies, including the possibility to achieve longer photon lifetime and smaller photonic disorder.

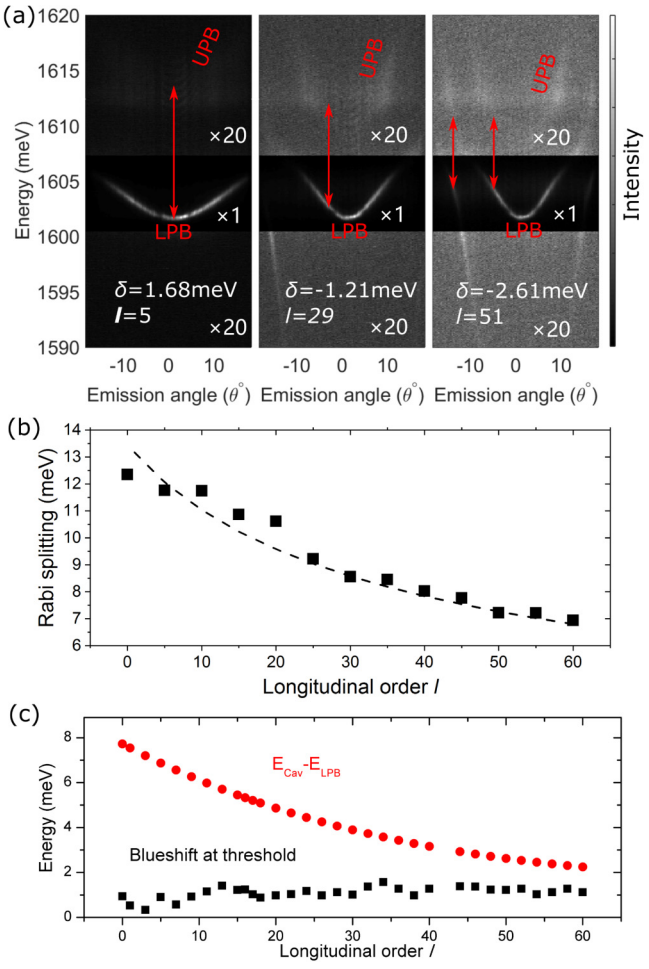

FIG. 2. (a) Emission intensity of the open-access cavity below lasing threshold (pump power = 200 μW) as a function of photon energy and emission angle for longitudinal orders l of 5 (left panel), 29 (middle panel), and 51 (right panel). The cavity-exciton detuning δ is shown for each graph, and the red arrows indicate the Rabi splitting. Intensity in some areas is multiplied by 20 for better visibility. (b) Experimental data (black squares) and theoretical fitting (dashed line) of the Rabi splitting as a function of l. (c) LPB blueshift (black squares) and the energy difference between the bare cavity and LPB bottom (red circles) for each l, while the LPB bottoms are fixed at 1602 meV as in (a).

It is notable that the visibility of the UPB decreases with Rabi splitting. The UPB is clearly seen for $l = 51$, gets broader and dimmer for $l = 29$, and becomes hardly visible for $l = 5$ in which the Rabi splitting (∼12 meV) is comparable with the exciton binding energy. The decrease is probably due to more absorption associated with polariton scattering to high-k excitons and generation of free charges, which is consistent with the absence of UPB in the wide-bandgap inorganic, organic, and perovskite microcavities working in the strong coupling regime.[9,24–27] The unique advantage of the planar open-access system lies in that it provides a systematic approach to evaluate the UPB viability vs vacuum Rabi splitting through a large range of cavity longitudinal orders.

The relaxation mechanism for polaritons to reach condensation is governed by the balance between the particle thermodynamics and the relaxation kinetics. For a given Rabi splitting, positively detuned polaritons exhibit a faster scattering rate, a longer polariton lifetime, and a shallower energy trap in momentum space from the exciton reservoir, while negatively detuned polaritons have lower thermodynamic critical density for condensation due to smaller effective mass, which results in an optimum detuning at which the polariton lasing threshold reaches its minimum.[7] In previous studies, polariton condensation threshold diagrams were investigated at a series of temperatures in different systems.[7–10] Herein, we derive polariton condensation threshold diagrams at the same temperature but with different Rabi splittings at $l = 5$, 29, and 51 by measuring the condensation threshold as a function of LPB energy in Fig. 3(a), which is converted to cavity-exciton detuning in Fig. 3(b). Herein, the threshold is expressed using the effective pump power taking into consideration the interference of the pump beam inside the cavity, which varies with l (see supplementary materials). The observations show that the optimum detuning, being 1.68, −1.21, and −2.61 meV for $l = 5$, 29, and 51, respectively, shifts toward positive values with increasing Rabi, which agrees with the previous theoretical predictions.[28] A quantitative simulation using the kinetics vs thermodynamics model[7–9] that agrees well with the experimental results is

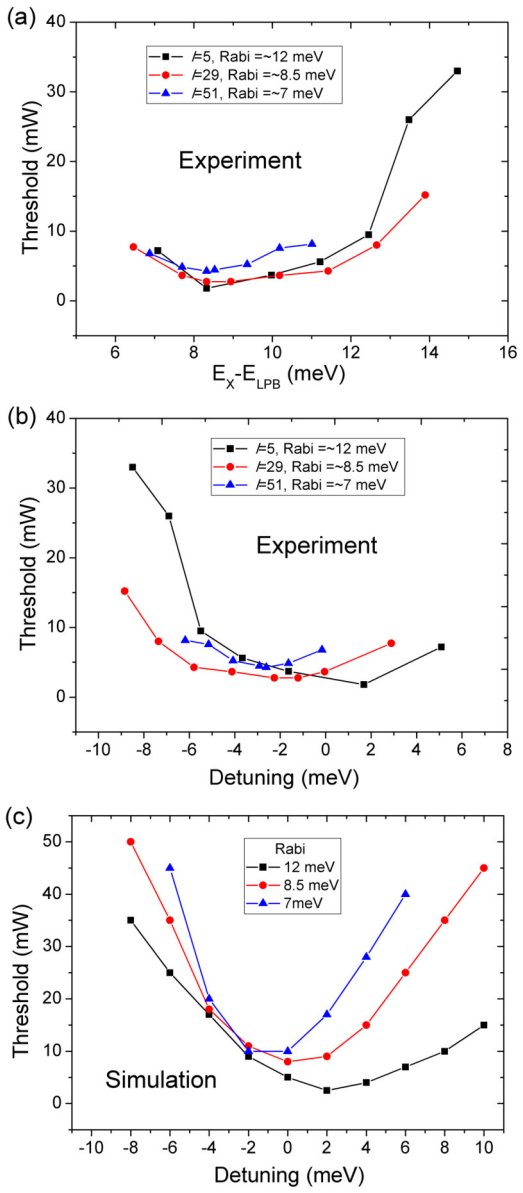

FIG. 3. Experimental results (a) and (b) and theoretical simulations [(c), The link between the injected exciton density (which is the model input) and the pumping power is made assuming a laser absorption per QW of 2%[29] and a perfect conversion from electron-hole pairs to excitons.] of polariton condensation threshold as a function of cavity-exciton detuning [(b) and (c)] and energy gap between the exciton and LPB bottom (a) at different Rabi splittings corresponding to cavity longitudinal orders $l = 5$, 29, and 51.

shown in Fig. 3(c). We note that for each l, the threshold minimum is the only one obtained both theoretically and experimentally, without any other appearing at more positive or negative detunings. The particular interest of varying the Rabi for the condensation threshold diagram lies in the capability to address the role of momentum-space potential trap independently of the particle properties such as the effective mass and the lifetime. Indeed, as displayed in Fig. 3(a), the optimum detunings of the three longitudinal orders all correspond to an energy gap between the LPB bottom and the exciton reservoir of 8.32 meV, indicating that the potential trap in momentum space, whose depth affects the efficiency of exciton–exciton scattering from high momenta exciton reservoir toward the polariton ground state, can be the key factor to determine the optimum detuning for polariton condensation in the drive-dissipative system. These results further support the earlier investigations of the condensation mechanism involving exciton-pair scattering with fixed Rabi splittings.[11]

IV. CONCLUSION

In conclusion, we established a planar open microcavity system that allows a large tuning range of Rabi splitting for 2D exciton–polaritons. Condensation is achieved and the corresponding threshold diagrams are derived for different longitudinal orders, which highlights the significant role of the momentum-space potential trap in the polariton condensation process. While extremely small mode volume is an intensely investigated area for nanophotonics, we show that, on the other hand, strong light–matter coupling and condensation can still be achieved with long cavities (cavity length up to $\sim 24\mu$m) provided the oscillator strength of the emitter is large enough. This reveals the potential to employ the advantages of long cavities, including larger cavity quality factor with the same reflectivity of mirrors and smaller photonic disorder with the same geometrical deformation compared to short cavities. These advantages are promising for fabricating arrays and lattices based on coupled open cavities without etching into the active layer,[30] which would be very difficult to achieve with short cavity length due to the slight geometrical difference among different concave mirrors. Our studies bridge the gap between micro- and macroscale cavities and pave the way for possible studies of polaritonics based on size-flexible cavities.

SUPPLEMENTARY MATERIAL

See the supplementary material for the details of the effective pump power.

ACKNOWLEDGMENTS

The authors acknowledge the National Natural Science Foundation of China (NNSFC) (Grant Nos. 12074303 and 11804267), Shaanxi Key Science and Technology Innovation Team Project (No. 2021TD-56); the support from the UK EPSRC under Grant Nos. EP/V026496/1 and EP/N031776/1 and from the megagrant No. 14.Y26.31.0015 of the Ministry of Education and Science of the Russian Federation; the support of the EU "TOPOLIGHT" project (No. 964770), of the ANR Labex Ganex (No. ANR-11-LABX-0014), and of the ANR program "Investissements d'Avenir" through the IDEX-ISITE initiative 16-IDEX-0001 (No. CAP 20-25).

AUTHOR DECLARATIONS

Conflict of Interest

The authors declare no conflict of interest.

DATA AVAILABILITY

The data that support the findings of this study are available from the corresponding author upon reasonable request.

REFERENCES

[1]M. S. Skolnick, T. A. Fisher, and D. M. Whittaker, Semicond. Sci. Technol. **13**, 645 (1998).
[2]H. Deng, H. Haug, and Y. Yamamoto, Rev. Mod. Phys. **82**, 1489 (2010).
[3]I. Carusotto and C. Ciuti, Rev. Mod. Phys. **85**, 299 (2013).
[4]K. J. Vahala, Nature **424**, 839 (2003).
[5]C. Weisbuch, M. Nishioka, A. Ishikawa, and Y. Arakawa, Phys. Rev. Lett. **69**, 3314 (1992).
[6]J. Ksprzaka, M. Richard, S. Kundermann, A. Baas, P. Jeambrun, J. M. J. Keeling, F. M. Marchetti, M. H. Szymanska, R. Andre, J. L. Staehli, V. Savona, P. B. Littlewood, B. Deveaud, and L. S. Dang, Nature **443**, 409 (2006).
[7]J. Kasprzak, D. D. Solnyshkov, R. André, L. S. Dang, and G. Malpuech, Phys. Rev. Lett. **101**, 146404 (2008).
[8]R. Butté, J. Levrat, G. Christmann, E. Feltin, J. F. Carlin, and N. Grandjean, Phys. Rev. B **80**, 233301 (2009).
[9]F. Li, L. Orosz, O. Kamoun, S. Bouchoule, C. Brimont, P. Disseix, T. Guillet, X. Lafosse, M. Leroux, J. Leymarie, M. Mexis, M. Mihailovic, G. Patriarche, F. Réveret, D. Solnyshkov, J. Zuniga-Perez, and G. Malpuech, Phys. Rev. Lett. **110**, 196406 (2013).
[10]O. Jamadi, F. Réveret, E. Mallet, P. Disseix, F. Médard, M. Mihailovic, D. Solnyshkov, G. Malpuech, J. Leymarie, X. Lafosse, S. Bouchoule, F. Li, M. Leroux, F. Semond, and J. Zuniga-Perez, Phys. Rev. B **93**, 115205 (2016).
[11]P. G. Savvidis, J. J. Baumberg, D. Porras, D. M. Whittaker, M. S. Skolnick, and J. S. Roberts, Phys. Rev. B **65**, 073309 (2002).
[12]E. M. Purcell, Phys. Rev. **69**, 37 (1946).
[13]R. Chikkaraddy, B. D. Nijs, F. Benz, S. J. Barrow, O. A. Scherman, and P. Fox, Nature **535**, 127 (2016).
[14]F. Li, Y. Li, Y. Cai, P. Li, H. Tang, and Y. Zhang, Adv. Quantum Technol. **2**, 1900060 (2019).
[15]P. R. Dolan, G. M. Hughes, F. Grazioso, B. R. Patton, and J. M. Smith, Opt. Lett. **35**, 3556 (2010).
[16]S. Dufferwiel, F. Fras, A. Trichet, P. M. Walker, F. Li, L. Giriunas, M. N. Makhonin, L. R. Wilson, J. M. Smith, E. Clarke, M. S. Skolnick, and D. N. Krizhanovskii, Appl. Phys. Lett. **104**, 192107 (2014).
[17]B. Besga, C. Vaneph, J. Reichel, J. Estève, A. Reinhard, J. Miguel-Sánchez, A. Imamoğlu, and T. Volz, Phys. Rev. Appl. **3**, 014008 (2015).
[18]R. T. Grant, R. Jayaprakash, D. M. Coles, A. Musser, S. De Liberato, I. D. Samuel, G. A. Turnbull, J. Clark, and D. G. Lidzey, Opt. Express **26**, 3320 (2018).
[19]L. Flatten, A. Trichet, and J. Smith, Laser Photonics Rev. **10**, 257 (2016).
[20]A. Muller, E. B. Flagg, J. R. Lawall, and G. S. Solomon, Opt. Lett. **35**, 2293 (2010).
[21]R. C. Pennington, G. D'Alessandro, J. J. Baumberg, and M. Kaczmarek, Phys. Rev. A **79**, 43822 (2009).
[22]P. M. Walker, L. Tinkler, B. Royall, D. V. Skryabin, I. Farrer, D. A. Ritchie, M. S. Skolnick, and D. N. Krizhanovskii, Phys. Rev. Lett. **119**, 097403 (2017), 1703.08351.
[23]D. N. Krizhanovskii, A. P. D. Love, D. Sanvitto, D. M. Whittaker, M. S. Skolnick, and J. S. Roberts, Phys. Rev. B **75**, 233307 (2007).
[24]S. Christopoulos, G. B. H. von Högersthal, A. J. D. Grundy, P. G. Lagoudakis, A. V. Kavokin, J. J. Baumberg, G. Christmann, R. Butté, E. Feltin, J. F. Carlin, and N. Grandjean, Phys. Rev. Lett. **98**, 126405 (2007).
[25]S. Kena Cohen and S. R. Forrest, Nat. Photonics **4**, 371 (2010).
[26]W. Xie, H. Dong, S. Zhang, L. Sun, W. Zhou, Y. Ling, J. Lu, X. Shen, and Z. Chen, Phys. Rev. Lett. **108**, 166401 (2012).
[27]R. Su, A. Fieramosca, Q. Zhang, H. S. Nguyen, E. Deleporte, Z. Chen, D. Sanvitto, T. C. H. Liew, and Q. Xiong, Nat. Mater. **20**, 1315 (2021).
[28]R. Johne, D. D. Solnyshkov, and G. Malpuech, Appl. Phys. Lett. **93**, 211103 (2008).
[29]M. V. Marquezini, J. Tignon, T. Hasche, and D. S. Chemla, Appl. Phys. Lett. **73**, 2313 (1998).
[30]S. Dufferwiel, F. Li, A. A. P. Trichet, L. Giriunas, P. M. Walker, I. Farrer, D. A. Ritchie, J. M. Smith, M. S. Skolnick, and D. N. Krizhanovskii, Appl. Phys. Lett. **107**, 201106 (2015).